Experimental and numerical study on the classification of a cyclonic field in a flotation column

Xiaoheng Li [1], Xiao Li [1], Xiaokang Yan [1,2], Lijun Wang [3], Haijun Zhang [1,2]

[1] School of Chemical Engineering and Technology, China University of Mining & Technology, Xuzhou, Jiangsu, 221116
[2] National Engineering Research Center of Coal Preparation & Purification, Xuzhou, Jiangsu, 221116
[3] School of Electric Power Engineering, China University of Mining & Technology, Xuzhou, Jiangsu, 221116

Corresponding author: xk-yan@cumt.edu.cn (Xiaokang Yan)

Abstract: The cyclonic-static micro-bubble flotation column (*FCSMC*) performs well in fine mineral flotation. Compared to traditional flotation columns, its design innovatively introduces a cyclonic structure. The separation of middling and tailing occurs in the cyclonic flow field induced by a cyclonic reversal cone. In this study, the particle size distribution analysis and computational fluid dynamics (*CFD*) simulations were conducted to reveal the particle distribution law and the classification mechanism in cyclonic flow fields under different circulation pressures. The results showed that particle size showed the same distribution tendency as tangential velocity in the radial direction: both increase from the center and decrease around the wall. As circulation flux increased, the tangential velocity increased, and the particle size differences in the radial direction also increased. The position of the largest particles will move to outside as the largest value of tangential velocity migrates the outward in the radial direction. According to the particle size distribution of the feed, it can be adjusted to the flow field to change the particle distribution, thereby improving the efficiency of separation. This study has an important guiding significance for column design and adjustment of the operating parameters of the flotation process.

Keywords: computational fluid dynamics, cyclonic flow field, cyclonic-static micro-bubble flotation column, particle size distribution

1. Introduction

With the continuous reduction of mineral resources, the demand for low-grade and complex ore has increased, leading to a lower size limit for flotation. Flotation column has been studied further because it achieves better separation for fine minerals. Harbort and Clarke (2017)divided the industrialization process of the flotation column into three phases, during which various types of flotation columns were tried and applied to industrial production. Through testing, more efficient flotation columns are retained, including the Jameson cell (Clayton et al., 1991), the Microcel (Yoon et al., 1992), the Pneuflot cell, the Cominco Engineering Services Ltd Column (*CESL*), and Cyclonic-static micro-bubble flotation column (*FCSMC*). The *FCSMC* was patented in 2000 (Liu, 2000). Plug flow, cyclonic flow, pipe flow, and jet flow were effectively combined in the column. Now, it has been applied in many fields such as mineral separation, oil-water separation, and decarbonization (Liu et al., 2013; Ran et al., 2013; Li et al., 2016) due to its excellent performance in fine minerals separation.

The structure of the *FCSMC* is shown in Fig. 1. The feed is introduced from the top of the column, and is separated through three stages, namely column flotation with low turbulence, cyclonic separation based on high-intensity centrifugal force field, and pipe mineralization with high turbulence. The combination of multiple flow patterns can overcome reduced floatability, and improves both mineralization and selectivity (Yan et al., 2018a). The working mechanism for the *FCSMC* has been thoroughly described in the literature (Zhang et al., 2013; Wang et al., 2015).

The column flotation zone has the advantages of a packed flotation column, and the packed sieve plate can change the flow pattern from a mono-turbulent circulating flow to a mild flow, thus effectively reducing the probability of particle detachment (Zhang et al., 2017; Yan et al., 2018b). Easily floatable particles can be concentrated by the rising bubble in this zone. Hard-floatable particles enter the pipe flotation zone. This section can increase turbulent kinetic energy and dissipation rate, increasing the possibility of bubble-particle collision and adhesion (Wang et al., 2017). The middling and the tailing particles were separated in the cyclonic flotation zone. In this zone, a cyclonic flow field was created by a reversal cone with a tangential inlet. Through the action of the centrifugal force field, the tailing and the middling particles were mainly classified according to the difference in particle size or density (Wang et al., 2015).

Industrial production is often troubled by the problem that the tailings cannot be effectively separated, leading to the loss of concentrate. However, less attention has been paid to the separation of middling and tailing particles in the cyclonic flow field, a process that directly affects the separation of the tailing. The separation is subject to the cyclonic flow field, but the manner in which the cyclonic flow field affects the classification is unclear. Therefore, in this study, we combined the particle size distribution experiment with Computational Fluid Dynamics (*CFD*) simulation to reveal the particle distribution law and the classification mechanism in this cyclonic flow field.
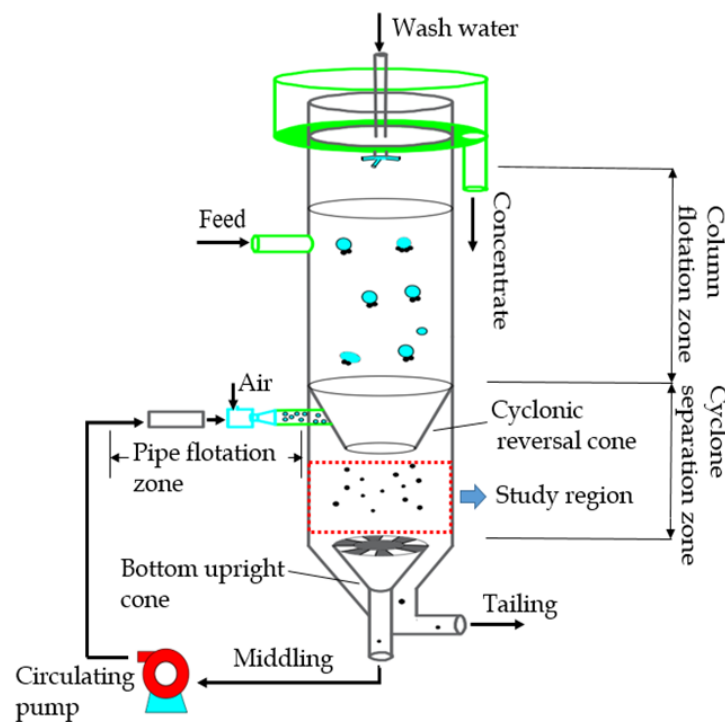

Fig. 1. Schematic of the cyclonic-static micro-bubble flotation column (*FCSMC*)

2. Experimental

2.1. Samples

Pure magnetite mineral particles with a density of 4960 kg/m^3 were used in the particle size distribution analysis. Particle size composition was measured by the US Microtrac S3500 Series Laser Particle Size Analyzer, as shown in Fig. 2.

2.2. Equipment and operating conditions

The distribution test system is shown in Fig. 3. The *FCSMC* used in this study had an inner diameter of 200 mm and a total height of 1800 mm. Mineral particles and water were well mixed in a mixing tank and then introduced into the column with a feed pump. The circulation pump drove slurry circulation under preset pressure. The experimental concentration was 1%, which was much smaller than the actual
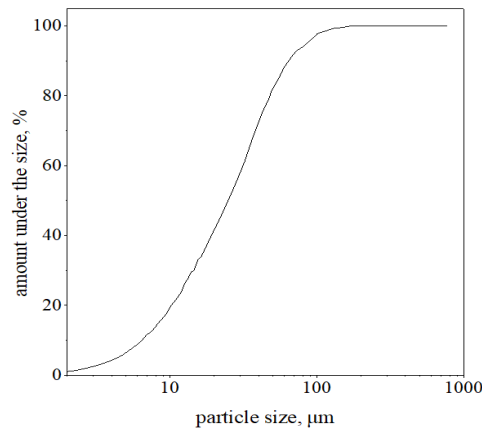
Fig. 2. Particle size distribution of magnetite sample

flotation, to ensure that the particle size distribution was more obvious. A pressure gauge (5) was installed at the outlet of the pump to record the pressure. The circulating pressure was equal to the pressure at the outlet of the pump in this study. The choice of circulating pressure (P_c) was within the scope of actual flotation. There were four experimental pressures: 0.1 MPa, 0.14 MPa, 0.18 MPa, and 0.22 MPa.
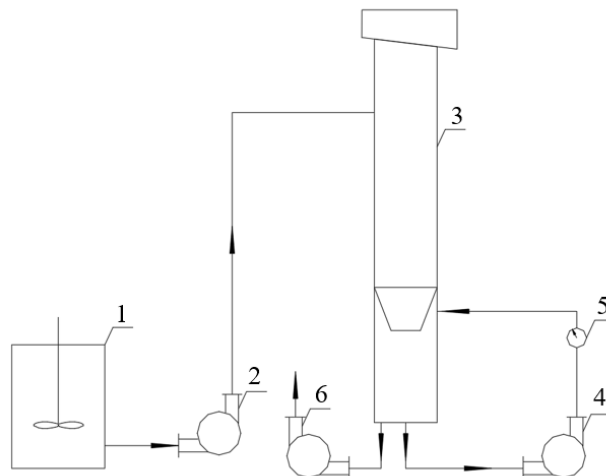

Fig. 3. The distribution test system of flotation column: (1) Mixing tank (2) Feed pump (3) *FCSMC* column (4) Circulation pump (5) Pressure gauge (6) Tailing pump

Five sampling heights were set in the axial direction: -128 mm (a) -188 mm (b) -248 mm (c) -308 mm (d) and -368 mm (e), as shown in Fig. 4. There were six sampling points in the radial direction for each height, and the values of r/R were 0, 0.2, 0.4, 0.6, 0.8, and 1.0. "0" indicated the center, and "1.0" was closest to the wall. Five retractable tubes were used to obtain samples. The collected samples were filtered and dried, and then its particle size composition was analyzed by laser particle size analysis. The sampling was conducted three times to obtain the average of the sample points reliable data, and the average particle size was calculated.

As the distribution curve is simple and similar, it noted that in the following text, the maximum difference of particle size in whole radial direction, $(\Delta d_p)_{max} = d_{pmax} - d_{pmin}$ (where d_{pmax} and d_{pmin} represent the maximum and minimum particle size in the radial direction, respectively), was calculated in order to evaluate the effect of classification performance in the radial direction.

2.3. Results and discussion

Fig. 5 shows the particle size distribution along the radial direction under four pressures. The distribution of particles in the radial direction is obvious for all sampling planes. First, the radial distribution of the particle size satisfies the particle distribution law that they will increase from the

center and decrease near the wall. Second, for the same P_c, in the axial direction, and the d_{pmax} appears in the same position. When P_c increases from 0.1 Mpa to 0.22 Mpa, the d_{pmax} appears at approximatively r/R = 0.4, 0.6, 0.6, 0.8. Namely, increasing the circulation pressure can promote the coarser particles to the outside.
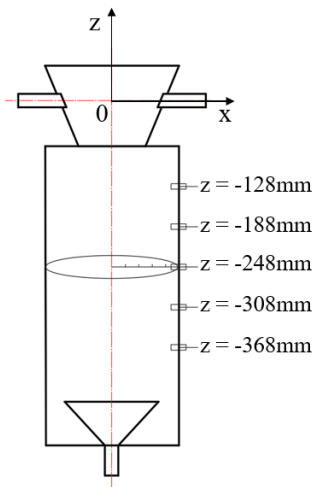

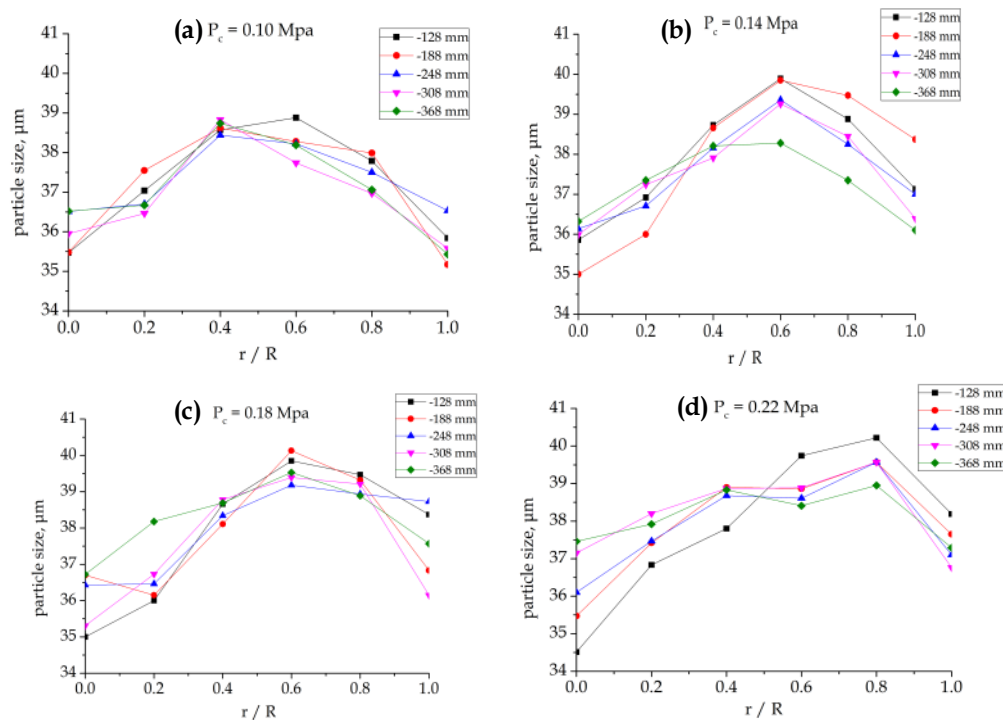Fig. 4. Sampling plane of column

Fig. 5. Particle size distribution for five sampling planes under different pressure (a) 0.10 Mpa, (b) 0.14 Mpa, (c) 0.18 Mpa, (d) 0.22 Mpa

Third, $(\Delta d_p)_{max}$ were figured out as shown in Fig. 6. As the P_c increased from 0.10 Mpa to 0.22 Mpa, at z = -128 mm, the sampling plane closest to the reversal cone, $(\Delta d_p)_{max}$ increases with the increase of circulation pressure, and the classification is enhanced. In other planes, there is no obvious law. Forth, under four working conditions, generally, the $(\Delta d_p)_{max}$ is gradually reduced downward in the axial direction, indicating that classification is weakening. d_{pmax} and d_{pmin} of each sampling plane under different pressures are shown in Fig. 7. Under the same P_c, the maximum particle size of the particles gradually decreases, and the minimum particle size gradually increases downwardly along the axial direction.
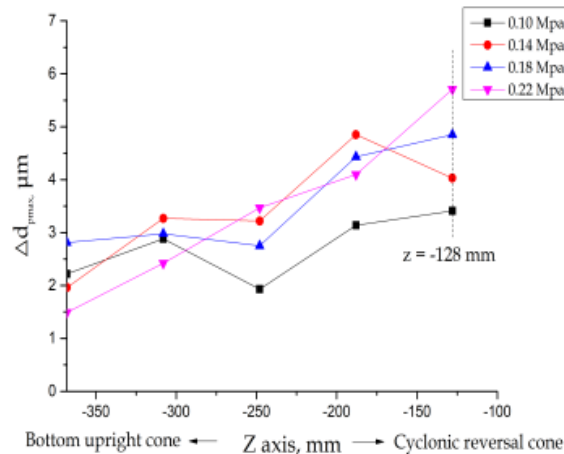
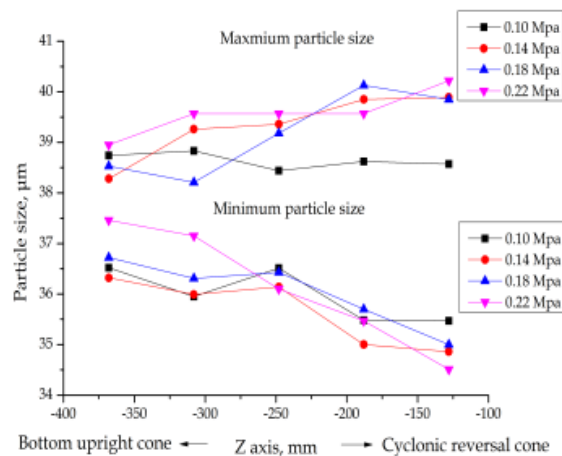Fig. 6. The $(\Delta d_p)_{max}$ for each sampling plane

Fig. 7. Maximum and minimum particle size of sampling planes under different pressure

3. Numerical simulation

The flow field of the flotation column was simulated in order to explore the relationship between the particle size distribution and the flow field.

3.1. *CFD* model

Structured grids were used for the simulation, as shown in Fig. 8. Grid independence test showed that 297000 grids were satisfied by the calculation, as shown in Fig. 9.

Existing *CFD* simulation studies on the flotation process are numerous, and many models have been discussed (Wang et al., 2018). Because the motion of the particles is mainly dominated by fluid flow, a single-phase flow field was used to predict the motion of the particles. Single-phase flow was simulated by FLUENT. The RSM model was chosen to calculate the turbulence flow. The boundary conditions for the upper outlet were defined as symmetric. Inlet and outlet velocities were adopted to maintain the flow balance, and the fluxes were the same as that measured under the experimental circulation pressure. Four fluxes were used: Q_1 = 2.32 m³/h (v_1 = 1.03 m/s), Q_2 = 2.64 m³/h (v_2 = 1.17 m/s), Q_3 = 3.0 m³/h (v_3 = 1.33 m/s), Q_4 = 3.34 m³/h (v_4 = 1.48 m/s). Simulation methods for devices of the same size have been described in detail, and the models have been verified by the particle image velocimetry (*PIV*) experiment in existing literature (Wang et al., 2015; Meng et al., 2019; Su et al., 2019). The list of boundary conditions and solution methods is presented in Table 1.
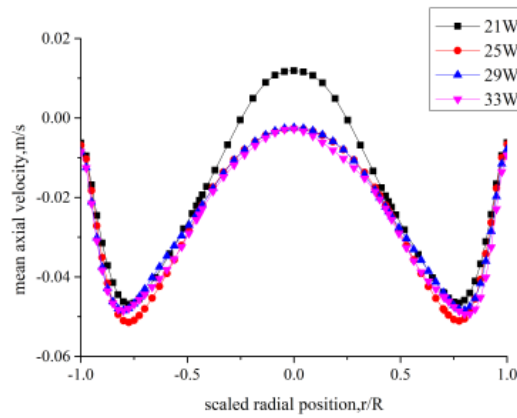
Fig. 8. Grid model

Fig. 9. Grid independence verification result

Table 1. Boundary conditions and solution methods

Turbulence model		RMS
Boundary conditions	Inlet	Velocity for cyclonic inlet
	Outlet	Velocity for the middling outlet
		Pressure for concentrate outlet
Solution methods	Pressure -Velocity coupling scheme	Simple
	The spatial discretization schemes	Least Squares Cell-Based for
		PRESTO! Scheme for pressure discretization
		Second-Order for momentum

3.2. Simulation results

3.2.1. Flow in a flotation column

Fig.10 shows the streamline inside the flotation column. Fluid rotates upward along the wall surface from the cyclonic cone. When the fluid reaches the top of the flotation column, it moves downward and

eventually enters the upright cone of the middling outlet. The streamline inside the cyclonic flow field is shown in Fig. 11. In the cyclonic flow field, after flowing out of the cyclonic reversal cone, the fluid expands toward the wall due to the centrifugal field. Limited by the wall and bottom outlet suction, the fluid rotates into the semi-open outlet of the bottom upright cone. In this process, the particles are classified: coarse particles enter the tailings outlet, and fine particles enter the middling outlet.
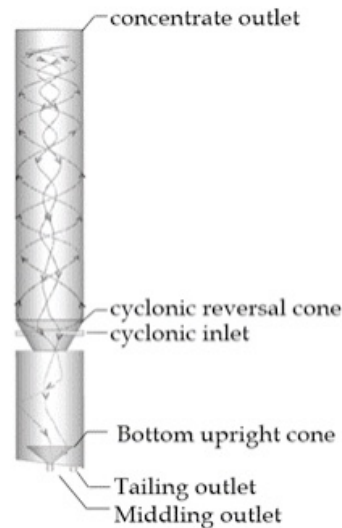

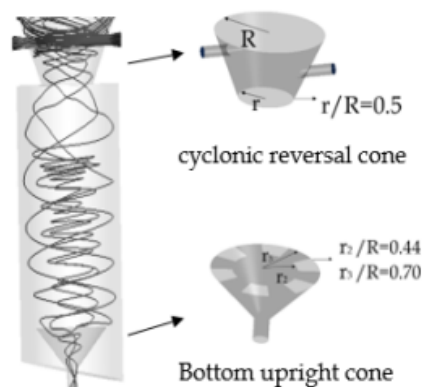Fig. 10. Streamline inside the flotation column

Fig. 11. Streamline inside cyclonic flow field

3.2.2. Velocity distribution in a cyclonic flow field

Fig. 12(a) shows the axial distribution contours under different fluxes. With the suction of the circulating pump, the main flow moves downward. The axial velocity of the fluid in the middle part of the column is upward due to the effect of "overflow" inside the cyclonic reversal cone and the blocking of the bottom baffle. The velocity increases with the increase of the circulation fluxes. When the circulation flux increases from Q_1 to Q_4, the axial velocity increases from - 0.05 m/sec to - 0.1 m/sec near the outlet of the cyclonic reversal cone.

Fig. 12(b) shows that in the main flow area, the radial velocity is small. At the outlet of the bottom upright cone, there is a slight local increase in radial velocity, between - 0.05 m/sec and - 0.1 m/sec.

Fig. 12(c) shows that the value of the tangential velocity is greater than the axial velocity and radial velocity, mainly between - 0.15 m/sec and - 0.20 m/sec. Under the same flux, the tangential velocity distribution is similar for all sampling planes, first increasing and then decreasing near the wall in the radial direction. In the axial direction, the change of tangential velocity is small for the same radial position between z = - 120 mm and z = - 360 mm. As the circulation flux increases, the tangential velocity in the flow field also increases.
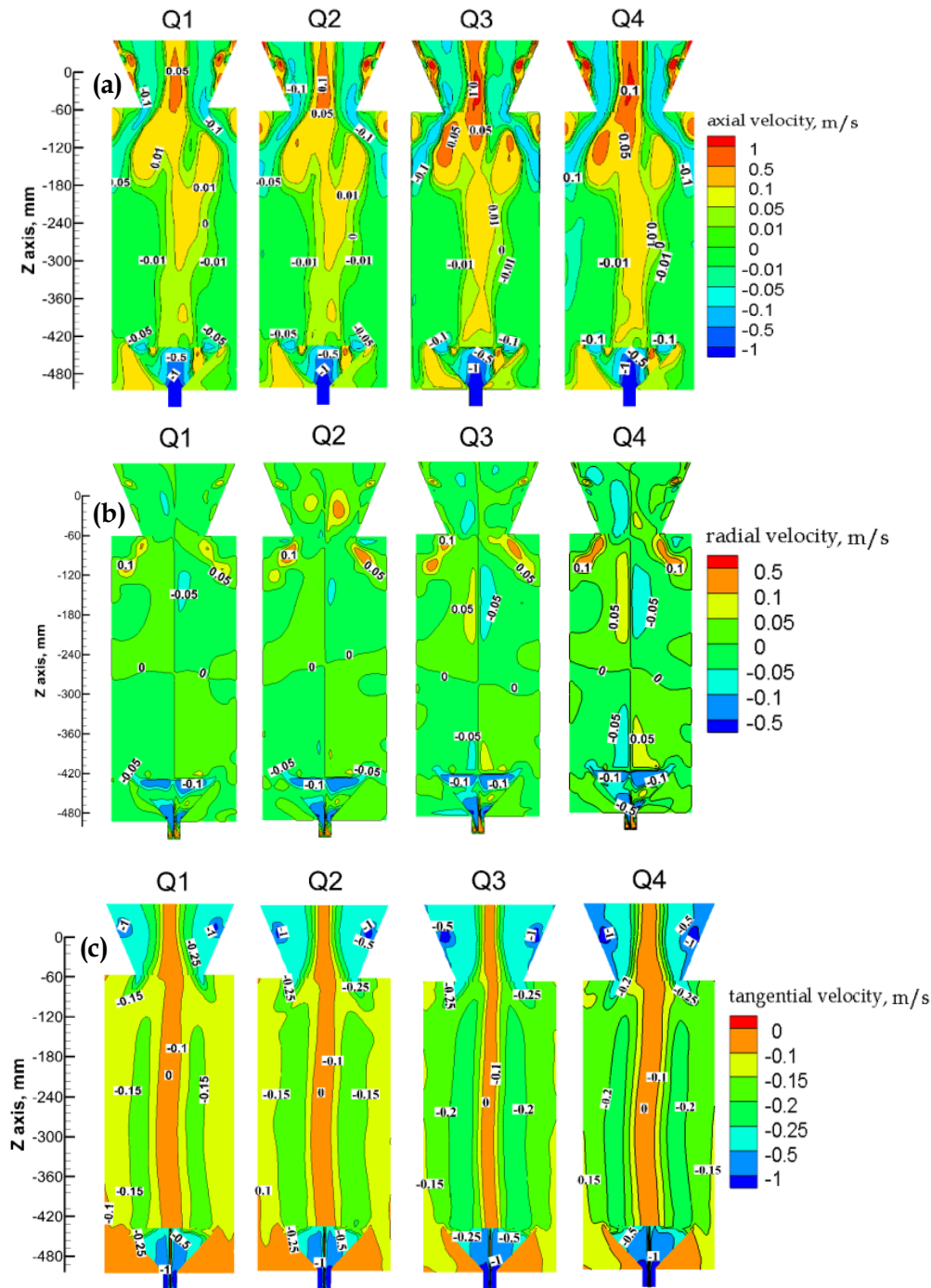
Fig. 12. Axial (a), radial (b) and tangential (c) velocity distribution under different fluxes

3.2.3. Relationship between velocity distribution and particle size distribution

As can be seen from Fig. 12(c), the value of the tangential velocity increases from the center and then decreases near the wall. Quantitatively, under the flux of Q_1, we figured the tangential velocity distribution of each sampling plane in Fig. 13. In the radial direction, it can be seen that the tangential velocity has a similar distribution tendency for all sampling planes, and the maximum velocity value is in almost the same radial position. It can be found that the tangential velocity and the particle size have the same distribution in the radial direction.

The plane of Z = -128 mm was selected to analyze the change of tangential velocity with flux, as shown in Fig. 14. When the circulation flux increases from Q_1 to Q_4, the tangential velocity on the outside increases markedly. Higher tangential velocity means a stronger centrifugal force field. Smaller particles

will enter the overflow, and larger particles will move toward the wall. Thus when flux increases, the maximum difference between particle sizes in the radial direction will also increase, which accords with the third conclusion in section 2.3.

Also, as the flux increases, the radial position of the maximum tangential velocity value moves from a to b, and the maximum tangential velocity increases from -0.14 m/sec to -0.20 m/sec. The largest particles move outward in the radial direction with the increase of circulation pressure.
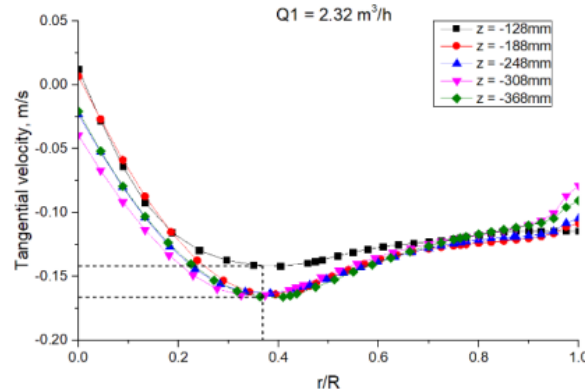

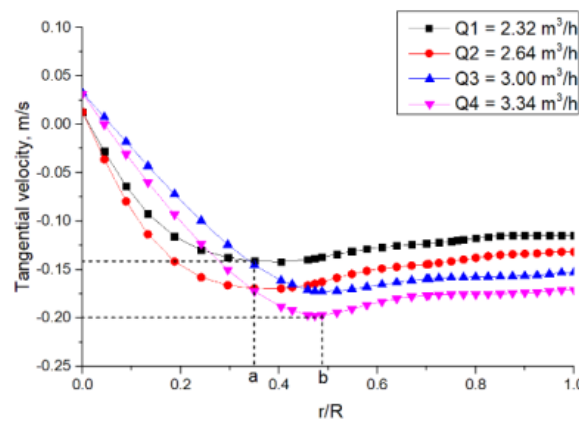Fig. 13. Tangential velocity distribution under Q_1 flux column

Fig. 14. Change of tangential velocity with flux on sampling plane of z = -128 mm

The above-mentioned analysis shows that the tangential velocity dominates the classification process. However, the forth conclusion in section 2.3 shows that the radial particle size difference decreases from the sampling plane Z = -128 mm to Z = -368 mm, while there is no obvious change in tangential velocity. As shown in Fig. 11 and Fig. 12 (b), When the fluid flows downward, affected by the suction of the bottom upright cone, in the axial direction, the streamline shrinks towards the bottom middling outlet. This radial movement of the fluid reduces the centrifugal force, thus the classification effect is weakened.

4. Further discussion

In mineral processing, two or more minerals are often embedded together, and liberation is required. Due to the difference in physical and chemical properties, the grindability of different mineral-rich ores varies, hence the size of the minerals is not the same. Particle size classification is quite important to improve separation performance. It can be seen from the above conclusion that particle size distribution is mainly subject to the tangential velocity, while the tangential velocity distribution in the cyclonic flow field is restricted by circulation pressure, the structure of the bottom upright cone and the cyclonic reversal cone. Therefore, we can get the following control strategies.

From the above-mentioned analysis, the coarsest particle size does not appear at the maximum radius of the column as usual thinking, and the position changes with the increase of circulation

pressure, therefore the design of the bottom upright cone at the bottom is particularly important. If the diameter is too large, coarse particles may enter the bottom upright cone and re-enter the cyclonic section, resulting in the reduction of separation efficiency; if the radius is too small, the mineral is easily lost in the tailings.

When the pressure is increased, the maximum difference of particle size in radial direction will also increase. For the feed, if the size of the target mineral particle is small, increasing the circulation pressure can enhance the classification process and promote the discharge of large particles. This has been proved by literature (Li et al., 2011), Li conducted flotation experiments, and found that the amount of magnesium with large size in tailings under the conditions of cyclonic circulation is obviously higher than that under direct-flow circulation in tailings. On the contrary, If the particle size or density of the target mineral is large, reducing the circulation pressure may weaken the classification process to avoid the loss of coarse particles.

Tangential velocity is affected not only by the circulating pressure, but also by the structure of the cyclonic reversal cone. Therefore, the angle is particularly important, and needs further study.

5. Conclusions

In this study, particle size distribution analysis and flow field *CFD* simulations of a small flotation column under different fluxes were performed. The particle distribution law and characteristics of flow field distribution in the cyclonic flow field were revealed. The relationship between them was analyzed, and the classification mechanism was explored. The main conclusions are as follows:

(1) The size of particles first increased and then decreased near the wall in the radial direction. Tangential velocity showed the same distribution tendency with particle size.
(2) As the circulation pressure increased, the largest particles moved outward in the radial direction. The maximum value of tangential velocity also migrated outward in the radial direction.
(3) In the downward axial direction, the particle size difference in the radial direction gradually reduced. The effect of the classification of particles gradually weakened.
(4) The difference between particle sizes in the radial direction increases with the increase of circulation pressure at the sampling plane of Z = -128 mm, which is closest to the cyclonic reversal cone. When the circulation flux increases from Q_1 = 2.32 m³/h to Q_4 = 3.34 m³/h, the tangential velocity markedly increases, indicating that the centrifugal force field is enhanced, and classification in the radial direction is promoted.

The above-mentioned conclusion shows that particle size distribution is strongly affected by tangential velocity, thus we can control the flow field by adjusting the structure of the column and the operating parameters, to change the tangential velocity distribution, and then changing the distribution of the particle sizes. For instance, the increase in the circulation pressure would promote the coarse particles to move outward, thereby enhancing the effects of classification. Reducing the diameter of the bottom upright cone is beneficial for the discharge of coarse particles.

Acknowledgments

References

CLAYTON, R., JAMESON, G. J., MANLAPIG, E.V., 1991. *The development and application of the Jameson cell*. Minerals Engineering, 4(7-11), 925-933.

HARBORT, G., CLARKE, D., 2017. *Fluctuations in the popularity and usage of flotation columns – An overview*. Minerals Engineering, 100, 17-30.

LI, G., LIU, J., CAO, Y., WANG, D., 2011. *Effect of a cyclonic flotation column on the separation of magnesium from phosphate ore*. Mining Science and Technology (China), 21(5), 647-650.

LI, X., XU, H., LIU, J., ZHANG, J., LI, J., GUI, Z., 2016. *Cyclonic state micro-bubble flotation column in oil-in-water emulsion separation*. Separation & Purification Technology, 165, 101-106.

LIU, J. (2000). *Cyclonic-static micro-bubble floatation apparatus and method*. United States Patent No. 6073775.

LIU, J., XU, H., LI, X., 2013. *Cyclonic separation process intensification oil removal based on microbubble flotation.* International Journal of Mining Science and Technology, 23(3), 415-422.

MENG, S., LI, X., YAN, X., WANG, L., ZHANG, H., CAO, Y., 2019. *Turbulence Models for Single Phase Flow Simulation of Cyclonic Flotation Columns.* Minerals, 9(8), 464.

RAN, J., LIU, J., ZHANG, C., WANG, D., LI, X. 2013. *Experimental investigation and modeling of flotation column for treatment of oily wastewater.* International Journal of Mining Science and Technology, 23(5), 665-668.

SU, W., YAN, X., WANG, L., ZHANG, H., CAO, Y., 2019. *Effect of height of flotation column on flow field.* Asia-Pacific Journal of Chemical Engineering, 14(3).

WANG, A., YAN, X., WANG, L., CAO, Y., LIU, J., 2015. *Effect of cone angles on single-phase flow of a laboratory cyclonic-static micro-bubble flotation column: PIV measurement and CFD simulations.* Separation & Purification Technology, 149, 308-314.

WANG, G., GE, L., MITRA, S., EVANS, G.M., JOSHI, J.B., SONG, C., 2018. *A review of CFD modeling studies on the flotation process,* Minerals Engineering, 127, 153-177.

WANG, L., WANG, Y., YAN, X., WANG, A., CAO, Y.J., 2017. *A numerical study on efficient recovery of fine-grained minerals with vortex generators in pipe flow unit of a cyclonic-static micro bubble flotation column.* Chemical Engineering Science, 158, 304-313.

YAN, X., MENG, S., WANG, A., WANG, L., CAO, Y., 2018a. *Hydrodynamics and separation regimes in a cyclonic–static microbubble flotation column.* Asia-Pacific Journal of Chemical Engineering, 13(13).

YAN, X., CHEN, Z., WANG, L., 2018b. *Computational fluid dynamics (CFD) numerical simulation and particle image velocimetry (PIV) measurement of a packed flotation column.* Physicochemical Problems of Mineral Processing, 54(2), 395-405.

YOON, R.H., LUTTRELL, G.H., ADEL, G.T., MANKOSA, M.J., 1992. *The Application of MicrocelColumn Flotation to Fine Coal Cleaning.* Coal Preparation, 10, 177-188.

ZHANG, H., LIU, J., WANG, Y., CAO, Y., MA, Z., LI, X., 2013. *Cyclonic-static micro-bubble flotation column.* Minerals Engineering, 45(5), 1-3.

ZHANG, M., LI, T., WANG, G., 2017. *A CFD study of the flow characteristics in a packed flotation column: Implications for flotation recovery improvement.* International Journal of Mineral Processing, 159, 60-68.